DOI: 10.1002/anie.201204006

Supramolecular Networks

Hierarchical Self-Assembly of Polycyclic Heteroaromatic Stars into Snowflake Patterns**

Stefan-S. Jester, Eva Sigmund, Lisa M. Röck, and Sigurd Höger**

Molecular self-assembly has been established as a key concept for the formation of functional monolayer patterns decorating solid surfaces. The field of two-dimensional (2D) crystal engineering relates the adlayer structure with the nature of the substrate and with the geometry and functionality of the adsorbed molecules. Shape-persistent molecules having a one-dimensional (1D; rigid rod oligomers)[1] or two-dimensional (polycyclic aromatic hydrocarbons (PAHs)[2] as well as rigid macrocycles)[3] structure and carrying flexible alkyl/alkoxy side chains have attracted considerable attention recently. They are adjustable in size with atomic-scale precision and can contain various functionalities. Moreover, the geometries and lattice dimensions of the surface patterns are transferred to the functional unit arrangements, thus giving rise to potential applications in single-molecule-based devices. However, to address that functionality on a single-molecule level by existing lithographic techniques, the amplitude of these structures has to have mesoscopic dimensions. A key problem is that the lattice parameters are generally close to the size of the molecules, and the time and effort required for the synthesis of defined molecules of that size is rather high.

Several self-assembly approaches are therefore explored to obtain 2D superstructures with large (tens of nanometers) lattice constants, and the approaches are based on either the homo- or co-assembly of molecules. In most cases, strong and directional noncovalent intermolecular interactions such as hydrogen bonding, dipole–dipole interaction, or metal coordination are the driving forces for the attraction between the molecules adsorbed to a (metal) surface.[4] Additionally, porous network structures and densely packed multicomponent architectures with large lattice constants have been obtained by utilizing intermolecular alkyl-chain interactions on highly oriented pyrolytic graphite (HOPG).[5] To maximize these interactions, adjacent alkyl chains on the same side of the molecule should be about 0.8–1.0 nm apart from each other, thus allowing their intermolecular interdigitation.[6] Intriguing examples are triangular phenylene–ethynylene macrocycles bearing two alkoxy substituents on each aromatic corner unit, which fulfills these size requirements ideally (the distance between the alkoxy chains of neighboring benzene rings measures 0.98 nm), and their symmetry matches perfectly with the underlying substrate.[5a]

However, despite considerable progress in the understanding of the basic principles that govern the 2D self-assembly of such molecules, the creation of surface patterns by a single component with more than one or a few molecules in the unit cell based on pure van der Waals interactions is still in its infancy.[7]

In this work we describe D_{3h}-symmetric polycyclic heteroaromatic structures with alkoxy chains of different lengths and their self-organization on HOPG (Figure 1). The compounds are rather easily accessible by condensation of hexaamino triphenylene with dialkoxyphenanthrene quinones. All molecules contain six alkoxy side groups with O–O distances of 0.99 nm for oxygen atoms on the same dibenzoquinoxaline unit and 0.95 nm for oxygen atoms framing the molecular bay regions. The orientation of the side chains of this rigid structure is widely adaptable and coordination numbers (CNs) from two to six can be adopted for the interaction (through side chains) with neighboring molecules (Figure 2a).[8] Depending on the specific orientation of the long flexible substituents, two, one, or no side chains of adjacent molecules may interdigitate (Figure 2b,c). We therefore expected a packing behavior of the molecules that would lead to long-range ordered networks. Our study was motivated by the question as to how structural motifs of the adlayer patterns vary with the chain length, $n = 10$–14, 16.

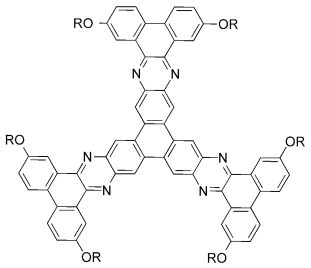

$[\mathbf{1}]_n$: R = C_nH_{2n+1}; n = 10–14, 16

Figure 1. Chemical structures of the star-shaped molecules $[\mathbf{1}]_n$; n defines the length of the alkoxy side chains.

Scanning tunneling microscopy (STM) investigations of adlayer patterns of $[\mathbf{1}]_n$ were performed at the interface of 1,2,4-trichlorobenzene (TCB) and HOPG. In all images, regions covered with conjugated backbones and alkoxy side chains are observed with high and low tunneling current,

[*] Dr. S.-S. Jester, Dr. E. Sigmund, L. M. Röck, Prof. Dr. S. Höger
Kekulé-Institut für Organische Chemie und Biochemie
Rheinische Friedrich-Wilhelms-Universität Bonn
Gerhard-Domagk-Strasse 1, 53121 Bonn (Germany)
E-mail: stefan.jester@uni-bonn.de
hoeger@uni-bonn.de

[**] Financial support by the DFG, the SFB 624, and the VolkswagenStiftung is gratefully acknowledged.

Supporting information for this article is available on the WWW under http://dx.doi.org/10.1002/anie.201204006.

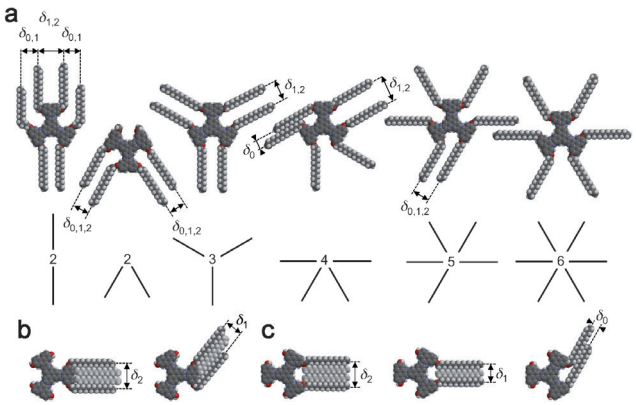

Figure 2. a) Selected examples of molecular models for $[\mathbf{1}]_n$ (here: $n=16$), thus illustrating different relative orientations of the alkoxy side chains and related side chain coordination numbers (CN = 2–6). b,c) Alkoxy side-chain interdigitation motifs for $[\mathbf{1}]_n$. Two, one, or no side chain (brightly grey, from adjacent molecules) interdigitating with two side chains framing a dibenzoquinoxaline unit (b) and a bay region (c) of $[\mathbf{1}]_n$. The latter consequently adopt distances δ_2, δ_1, and δ_0.

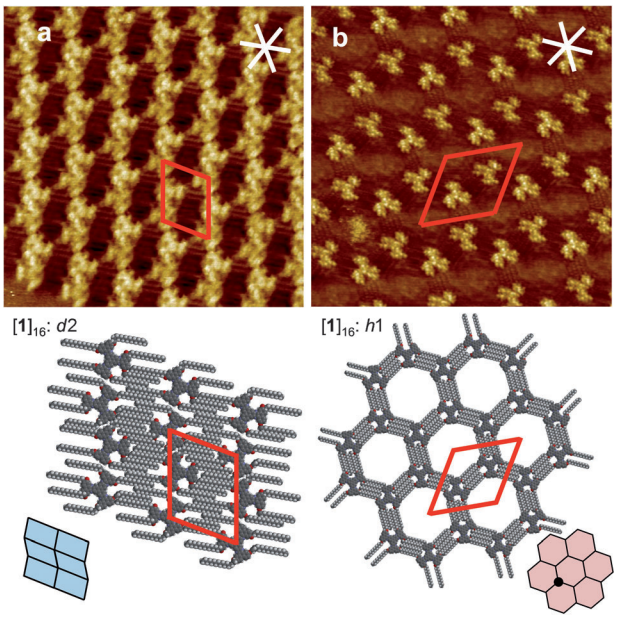

Figure 3. STM images as well as molecular and schematic models of the a) dense (*d2*) and b) porous (*h1*) patterns of $[\mathbf{1}]_{16}$ at the TCB/HOPG interface. For (a): *d2*: 26.3×26.3 nm^2; $c=2\times10^{-6}$ M, $V_S=-0.8$ V, $I_t=8$ pA; $a=(4.8\pm0.2)$ nm, $b=(4.3\pm0.1)$ nm, $\gamma(a,b)=(67\pm2)°$; p1; for (b): *h1* ((6^3) tiling): 25.7×25.7 nm^2; $c=10^{-6}$ M, $V_S=-0.6$ V, $I_t=6$ pA; $a=(6.0\pm0.2)$ nm, $b=(5.9\pm0.2)$ nm, $\gamma(a,b)=(61\pm2)°$; p6. The red and white lines denote unit cells and HOPG main axis directions, respectively.

which are encoded in bright and dark colors, respectively.[9] All adsorbed alkoxy side chains which contribute to the packing are oriented along the directions of the main axes of the HOPG substrate.[6] Depending on the concentration and sample preparation parameters, all compounds form domains of distinct dense and porous polymorphs.

With the exception of $[\mathbf{1}]_{13}$, all compounds $[\mathbf{1}]_n$ self-assemble into densely packed oblique surface patterns (plane group p1) which can be viewed as dumbbell-shaped pairs of molecules ($n=10$, 11; denoted as *d1*) or rows of alternately oriented molecules ($n=12$, 14, 16; named *d2*) separated by interdigitating alkoxy side chains, thus showing that the overall packing concept of the backbones is maintained throughout all chain lengths. A dense pattern for $[\mathbf{1}]_{16}$ is representatively shown in Figure 3a.

Simultaneously, $[\mathbf{1}]_n$ where $n=13$, 14, and 16, form porous hexagonal adsorbate patterns (denoted as *h1*, plane group p6) with identical packing but different backbone distances, depending on the side-chain length. Representatively for the *h1* patterns, an STM image and the packing model of $[\mathbf{1}]_{16}$ are shown in Figure 3b. Two alkoxy side chains (i.e., framing the bay regions) of two dibenzoquinoxaline units of each molecule are aligned in parallel. All bay regions of adjacent molecules point towards each other so that four alkoxy side chains interdigitate. In such way, each molecule is connected to three adjacent molecules (CN = 3) so that the polycyclic heteroaromatic backbones are separated from each other. The resulting pores can be viewed as hexagonal honeycombs where the backbones (representing the corners) are connected by the alkoxy chains (forming the sides). The resulting cavity diameters vary from 4.4 to 5.3 nm (corner to opposite corner), and their distances range from 5.3 to 6.0 nm (pore center to pore center). In a schematic approach aiming at a more abstract description, the pattern is reduced to a honeycomb line grid where each crossing point (vertex) is formed by three adjacent regular hexagonal tiles (see Figure 3b and the Supporting Information). By adapting a nomenclature that was introduced in discrete geometry for *k*-uniform tilings we denote the *h1* pattern as (6^3) tiling.[10,11a,12,13]

For $[\mathbf{1}]_n$, where $n=10$, 12, a different hexagonal adsorbate pattern (denoted as $h2_2$, with a plane group p6) is observed (Figure 4a and the Supporting Information). At first glance this structure (again) appears to be a pattern of honeycomb-shaped nanopores, each formed by six (here densely packed) aromatic backbones of the molecules. The (hexagonal) nanopores are separated from each other by alkoxy side chains and are 7.5 nm ($[\mathbf{1}]_{10}$) and 7.8 nm ($[\mathbf{1}]_{12}$) apart (Table 1). Alternatively, the pattern can be viewed as densely packed triangular molecular assemblies, each of which consists of three molecules at the corners which interact through interdigitating alkoxy side chains, thus forming triangular pores in their inside. Four of the six alkoxy side chains of each molecule interact with (side chains of) adjacent molecules in two directions (with an angle of 60°) so that a CN = 2 (Figure 5a) occurs. The remaining side chains are disordered in the nanopore or point into the solution phase. Consequently, hexagonal pores of densely packed backbones can even be formed without having functional groups elsewhere to facilitate a directed interaction, for example, carboxylic acids.[14] The observation that $[\mathbf{1}]_n$ ($n=13$, 14, 16) forms the *h1* pattern while $[\mathbf{1}]_n$ ($n=10$, 12) forms the $h2_2$ pattern can be rationalized by a higher tendency of the longer side chains to be completely adsorbed to the graphite at the cost of a lower surface coverage.[5a] The fact that $[\mathbf{1}]_n$ can form hexagonal (*h1* pattern) as well as hexagonal and triangular pores ($h2_m$

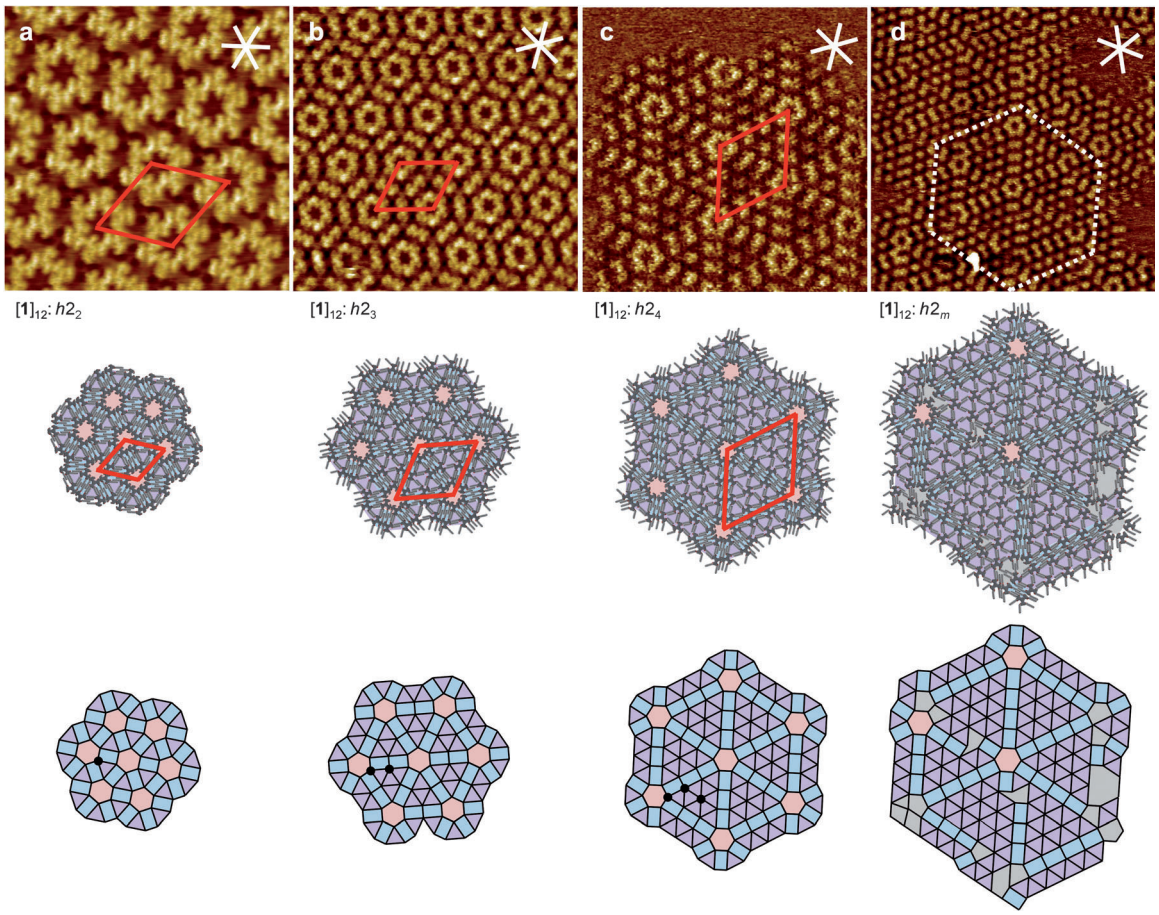

Figure 4. a–d) STM images as well as molecular and schematic models of the porous adlayer patterns $h2_m$ ($m=2$–4) and varying m (also $m=5$) for $[\mathbf{1}]_{12}$ at the TCB/HOPG interface. For (a): $h2_2$ (3.4.6.4): 28.5×28.5 nm^2, $c=5\times10^{-6}$ M, $V_S=-1.2$ V, $I_t=18$ pA, $a=(7.8\pm0.2)$ nm, $b=(7.8\pm0.2)$ nm, $\gamma(a,b)=(60\pm2)°$; p6; for (b): $h2_3$ ($3^3.4^2$; 3.4.6.4): 55.5×55.5 nm^2, $c=3\times10^{-6}$ M, $V_S=-1.6$ V, $I_t=5$ pA; $a=(11.2\pm0.3)$ nm, $b=(10.9\pm0.3)$ nm, $\gamma(a,b)=(60\pm2)°$; p6; for (c): $h2_4$ (3^6; $3^3.4^2$; 3.4.6.4): 58.8×58.8 nm^2, $c=3\times10^{-6}$ M, $V_S=-1.0$ V, $I_t=18$ pA; $a=(15.5\pm0.3)$ nm, $b=(15.5\pm0.3)$ nm, $\gamma(a,b)=(60\pm2)°$; p6; for (d): $h2_m$: 86.1×86.1 nm^2, $c\approx10^{-6}$ M, $V_S=-1.2$ V, $I_t=20$ pA. The red and white lines denote unit cells and HOPG main axis directions, respectively. The white dotted hexagon in (d) indicates the region transcribed by the molecular model. The black dots in the line patterns of (a)–(c) point out distinct vertices of each tiling.[15]

Table 1: Pattern structures for $[\mathbf{1}]_n$ ($n=10$–14, 16), $[\mathbf{2}]_{16}$, and $[\mathbf{3}]_{16}$.

		a [nm]	b [nm]	γ [°]	N[a]
$[\mathbf{1}]_{10}$	$d1$	5.6 ± 0.2	3.2 ± 0.1	53 ± 2	2
	$h2_2$	7.5 ± 0.2	7.5 ± 0.2	60 ± 2	6
$[\mathbf{1}]_{11}$	$d1$	4.9 ± 0.2	3.9 ± 0.2	67 ± 2	2
	am.				
$[\mathbf{1}]_{12}$	$d2$	6.0 ± 0.1	3.8 ± 0.1	60 ± 2	2
	$h2_2$	7.8 ± 0.2	7.8 ± 0.2	60 ± 2	6
	$h2_3$	11.1 ± 0.3	11.1 ± 0.3	60 ± 2	12
	$h2_4$	15.5 ± 0.3	15.5 ± 0.3	60 ± 2	20
	$(h2_5)$[b]	(18.8±0.4)	(18.8±0.4)	(60±2)	(30)
$[\mathbf{1}]_{13}$	$h1$	5.3 ± 0.2	5.3 ± 0.2	60 ± 2	3
$[\mathbf{1}]_{14}$	$d2$	5.0 ± 0.2	4.1 ± 0.1	66 ± 2	2
	$h1$	5.8 ± 0.2	5.8 ± 0.2	60 ± 2	3
$[\mathbf{1}]_{16}$	$d2$	4.8 ± 0.2	4.3 ± 0.1	67 ± 2	2
	$h1$	6.0 ± 0.2	6.0 ± 0.2	60 ± 2	3
$[\mathbf{2}]_{16}$	d	4.7 ± 0.1	4.0 ± 0.1	76 ± 2	2
$[\mathbf{3}]_{16}$	$h3$	7.7 ± 0.2	7.7 ± 0.2	60 ± 2	6
	d'	4.9 ± 0.1	2.8 ± 0.1	90 ± 2	2
	d''	8.8 ± 0.2	5.1 ± 0.1	51 ± 2	4

[a] Molecules per unit cell. [b] Only observed in co-occurrence with other assemblies (of varying m); nominal unit cell given.

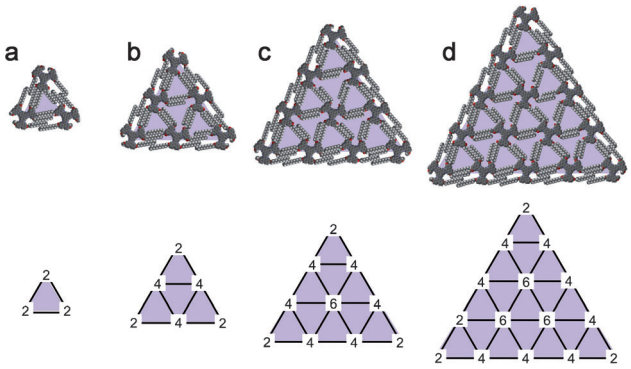

Figure 5. Molecular and schematic models of supramolecular aggregates showing the tiles of the adlayer patterns a) $h2_2$, b) $h2_3$, c) $h2_4$ (shown in Figures 4a–c, respectively), and d) $h2_5$ (only observed in random mixed patterns with varying m; see Figure 4d). The digits at the vertices of the line grids indicate coordination numbers of the respective molecular building blocks.[8,16]

patterns, here: $m=2$, where m describes the number of molecules that form the triangle side), both through side-chain interdigitation, is clearly a result of the adaptive behavior of the molecules with respect to number and direction of the interdigitating substituents. As discussed at the end of the previous paragraph, an abstraction towards a line network leads to vertices formed by triangular, rectangular, and hexagonal tiles, more precisely a (3.4.6.4) tiling (see Figure 4a and the Supporting Information).

Of special interest is the observation that the molecules $[\mathbf{1}]_{12}$ simultaneously form the "inflated" structures $h2_3$, $h2_4$, and $h2_5$ (Figure 4b–d).[4] In each case, another row with $n+1$ molecules is added to the triangle that—in the case of $h2_3$ and $h2_4$—forms half a unit cell (Figure 5). Within such a triangle the molecules are connected/linked by interdigitating alkoxy side chains. The coordination number of the molecules within the triangles depends on their position. Molecules at the corners are only connected to two other molecules (by alkoxy chain interdigitation; CN = 2), while molecules at the edges have the CN = 4, and molecules in the inner part of the triangle adopt CN = 6 (Figure 5a–d). These triangles are closely packed at the surface, and each triangle corner forms—with the corners of five adjacent triangles—a hexagonal pore as discussed before. The pore diameter (of 2.8 nm) is equal in all structures, while the pore distances range from 7.8 nm ($h2_2$) up to 15.5 nm ($h2_4$) and nominally 18.8 nm ($h2_5$), and consequently very large unit cells with 20 ($h2_4$) and nominally 30 ($h2_5$) molecules are indexed. The packing behavior of $[\mathbf{1}]_{12}$ is rather surprising. $[\mathbf{1}]_{16}$ forms a porous network of isolated molecules where all side chains are adsorbed to the surface, while $[\mathbf{1}]_{10}$ forms a network of triangular assemblies leading to a higher grafting density at the cost of the possibility for all alkoxy chains to lie on the graphite. In the case of $[\mathbf{1}]_{12}$ we are in the medium-chain-length regime. We did not observe only the expected coexistence of these two polymorphs in separate domains, but additionally we found adsorbate patterns which contain elements of both packing motifs and are combined into a frustrated structure. The molecules are able to assemble to superstructures that hierarchically form crystalline patterns with very large unit cells. For this superstructure formation, it is highly important that the side chains of the molecules are widely adaptable and a variety of distinct coordination numbers and interaction motifs become possible. A comparison with $[\mathbf{2}]_{16}$, which contains four long alkoxy side chains at two dibenzoquinoxaline units (Figure 6 and the Supporting Information), shows that it cannot form a porous network structure (like $[\mathbf{1}]_{16}$; Figure 3b), as the molecule lacks a threefold symmetry. In contrast, $[\mathbf{3}]_{16}$ has only two long alkoxy side chains enforcing the formation of trimeric clusters. These self-assemble, as expected, into a porous network similar to that of $[\mathbf{1}]_n$ ($n=10, 12$), $h2_2$, but no higher-ordered complex superstructures could be observed that require also building blocks with higher coordination numbers.[17]

Higher-order network structures have been observed for other C_3-symmetric molecules as a result of commensurability criteria of the adlayer and the substrate,[18] or through a combination of strong and directional forces (for example, hydrogen bonding).[4] In those cases the unit cells are connected by strong bonds, and the intermolecular bonds between the molecules within the unit cells are weaker.[4c]

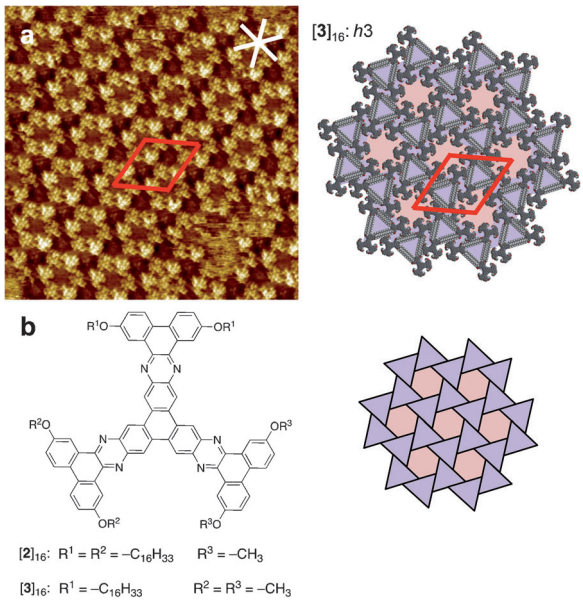

Figure 6. a) STM image as well as molecular and schematic models of an adlayer pattern of $[\mathbf{3}]_{16}$ at the TCB/HOPG interface (44.1×44.1 nm^2; $c=2\times10^{-4}$ M, $V_S=-1.0$ V, $I_t=5$ pA; $a=(7.7\pm0.2)$ nm, $b=(7.7\pm0.2)$ nm, $\gamma(a,b)=(60\pm2)°$; p6). The red and white lines denote unit cells and HOPG main axis directions, respectively. b) Chemical structures of $[\mathbf{2}]_{16}$ and $[\mathbf{3}]_{16}$.

In the case presented here, we show that higher-order honeycomb network structures with increasing interpore distance can also be observed for C_3-symmetric molecules purely by van der Waals attraction. A key element in these networks is the ability of the molecules to adapt the number and direction of the interdigitating substituents such that they can hierarchically build up complex superstructures.

Conclusively, we have described star-shaped polycyclic heteroaromatic molecules, substituted with six (four, two) alkoxy side chains. The length and number of the substituents determines which crystal patterns the molecules assemble into, and distinct packing motifs were observed for long and short side chains. For the intermediate-chain-length regime, a frustrated structure having very large unit cell parameters was observed. As far as we know this is the first time that such large superstructures of one compound on HOPG have been observed, wherein the molecules are held together only by van der Waals attraction. Ongoing studies focus on the question of the molecular requirements for the inflated structure formation and how this can be controlled.

Received: May 23, 2012
Revised: June 22, 2012
Published online: July 23, 2012

Keywords: hydrocarbons · interfaces · polycycles · scanning tunneling microscopy · self-assembly

[1] For self-assembled monolayers (SAMs) of shape-persistent linear oligomers, see: a) P. Samorí, N. Severin, K. Müllen, J. P. Rabe, *Adv. Mater.* **2000**, *12*, 579; b) J.-R. Gong, J.-L. Zhao, S.-B. Lei, L.-J. Wan, Z.-S. Bo, X.-L. Fan, C.-L. Bai, *Langmuir* **2003**, *19*, 10128; c) Z. Mu, X. Yang, Z. Wang, X. Zhang, *Langmuir* **2004**, *20*, 8892; d) Z.-Y. Yang, L.-H. Gan, S.-B. Lei, L.-J. Wan, C. Wang, J.-Z. Jiang, *J. Phys. Chem. B.* **2005**, *109*, 19859; e) J.-R. Gong, H.-J. Yan, Q.-H. Yuan, L.-P. Xu, Z.-S. Bo, L.-J. Wan, *J. Am. Chem. Soc.* **2006**, *128*, 12384; f) K. Yoosaf, P. V. James, A. R. Ramesh, C. H. Suresh, K. G. Thomas, *J. Phys. Chem. C* **2007**, *111*, 14933; g) M. Wielopolski, A. Atienza, T. Clark, D. M. Guldi, N. Martín, *Chem. Eur. J.* **2008**, *14*, 6379; h) D. Mössinger, S.-S. Jester, E. Sigmund, U. Müller, S. Höger, *Macromolecules* **2009**, *42*, 7974; i) Z. Mu, S. Lijin, H. Fuchs, M. Mayor, L. Chi, *Langmuir* **2011**, *27*, 1359.

[2] For recent publications about SAMs of PAHs with alkyl/alkoxy side chains, see: J. M. Mativetsky, M. Kastler, R. C. Savage, D. Gentilini, M. Palma, W. Pisula, K. Müllen, P. Samorì, *Adv. Funct. Mater.* **2009**, *19*, 2486.

[3] For SAMs of shape-persistent macrocycles, see: a) S. Höger, K. Bonrad, A. Mourran, U. Beginn, M. Möller, *J. Am. Chem. Soc.* **2001**, *123*, 5651; b) E. Mena-Osteritz, P. Bäuerle, *Adv. Mater.* **2001**, *13*, 243; c) D. Borissov, A. Ziegler, S. Höger, W. Freyland, *Langmuir* **2004**, *20*, 2781; d) V. Kalsani, H. Ammon, F. Jäckel, J. P. Rabe, M. Schmittel, *Chem. Eur. J.* **2004**, *10*, 5481; e) S. Lei, K. Tahara, F. C. De Schryver, M. Van der Auweraer, Y. Tobe, S. De Feyter, *Angew. Chem.* **2008**, *120*, 3006; *Angew. Chem. Int. Ed.* **2008**, *47*, 2964; f) F. Schlosser, V. Stepanenko, F. Würthner, *Chem. Commun.* **2010**, *46*, 8350; g) S. K. Maier, S.-S. Jester, U. Müller, M. M. Müller, S. Höger, *Chem. Commun.* **2011**, *47*, 11023.

[4] a) G. Pawin, K. L. Wong, K.-Y. Kwon, L. Bartels, *Science* **2006**, *313*, 961; b) Y. Ye, W. Sun, Y. Wang, X. Shao, X. Xu, F. Cheng, J. Li, K. Wu, *J. Phys. Chem. C* **2007**, *111*, 10138; c) W. Xiao, X. Feng, P. Ruffieux, O. Gröning, K. Müllen, R. Fasel, *J. Am. Chem. Soc.* **2008**, *130*, 8910; d) J. Zhang, B. Li, X. Cui, B. Wang, J. Yang, G. J. Hou, *J. Am. Chem. Soc.* **2009**, *131*, 5885; e) S. Clair, M. Abel, L. Porte, *Angew. Chem.* **2010**, *122*, 8413; *Angew. Chem. Int. Ed.* **2010**, *49*, 8237.

[5] a) K. Tahara, C. A. Johnson II, T. Fujita, M. Sonoda, F. C. De Schryver, S. De Feyter, M. M. Haley, Y. Tobe, *Langmuir* **2007**, *23*, 10190; b) K. Tahara, S. Okuhata, J. Adisoejoso, S. Lei, T. Fujita, S. De Feyter, Y. Tobe, *J. Am. Chem. Soc.* **2009**, *131*, 17583; c) J. Adisoejoso, K. Tahara, S. Okuhata, S. Lei, Y. Tobe, S. De Feyter, *Angew. Chem.* **2009**, *121*, 7489; *Angew. Chem. Int. Ed.* **2009**, *48*, 7353.

[6] a) T. Yang, S. Berber, J.-F. Liu, G. P. Miller, D. Tománek, *J. Chem. Phys.* **2008**, *128*, 124709; b) B. Ilan, G. M. Florio, M. S. Hybertsen, B. J. Berne, G. W. Flynn, *Nano Lett.* **2008**, *8*, 3160.

[7] S.-S. Jester, E. Sigmund, S. Höger, *J. Am. Chem. Soc.* **2011**, *133*, 11062.

[8] In the context of this work, coordination numbers are defined as numbers of directions along which the alkoxy side chains of adjacent molecules are adsorbed on the HOPG surface to interact interdigitatively.

[9] R. Lazzaroni, A. Calderone, J. L. Brédas, J. P. Rabe, *J. Chem. Phys.* **1997**, *107*, 99.

[10] Each molecular backbone is located at a vertex position. The alkoxy side chains link the backbones—similar as the polygon edges connect the vertices and thus define the tiles. For details see the Supporting Information.

[11] *k*-uniform tilings: a) J. Kepler, *Harmonices Mundi*, **1619**; b) D. M. Y. Sommerville, *Trans. Roy. Soc. Edin.* **1905**, *41*, 725 ($k=1$); c) O. Krötenheerdt, *Math.-Natur. Reihe* **1969**, *18*, 273; O. Krötenheerdt, *Math.-Natur. Reihe* **1970**, *19*, 19; O. Krötenheerdt, *Math.-Natur. Reihe* **1970**, *19*, 97 ($k=2$); d) D. Chavey, *Comp. Math. Appl.* **1989**, *17*, 147 ($k=3$).

[12] An overview is found in: B. Grünbaum, G. C. Shepherd, *Tilings and Patterns*, W. H. Freeman & Company, New York, **1986**.

[13] In a chemical context, this nomenclature was applied for a description of mesostructures of block copolymers. See: T. Asari, S. Arai, A. Takano, Y. Matsushita, *Macromolecules* **2006**, *39*, 2232; Y. Matsushita, *Macromolecules* **2007**, *40*, 771.

[14] a) M. Lackinger, S. Griessl, W. M. Heckl, M. Hietschold, G. W. Flynn, *Langmuir* **2005**, *21*, 4984; b) K. G. Nath, O. Ivasenko, J. A. Miwa, H. Dang, J. D. Wuest, A. Nanci, D. F. Perepichka, F. Rosei, *J. Am. Chem. Soc.* **2006**, *128*, 4212; c) K. G. Nath, O. Ivasenko, J. M. MacLeod, J. A. Miwa, J. D. Wuest, A. Nanic, D. F. Perepichka, F. Rosei, *J. Phys. Chem. C* **2007**, *111*, 16996; d) N. T. N. Ha, T. G. Gopakumar, R. Gutzler, M. Lackinger, H. Tang, M. Hietschold, *J. Phys. Chem. C* **2010**, *114*, 3531; e) V. V. Korolkov, S. Allen, C. J. Roberts, S. J. B. Tendler, *J. Phys. Chem. C* **2012**; DOI: org/10.1021/jp212388c.

[15] The average relative abundances θ_{rel} by the different polymorphs at $c=3\times10^{-6}$ M (adsorption at RT) are: $\theta_{rel}(d2)=64.1\,\%$; $\theta_{rel}(h2_2)=6.8\,\%$; $\theta_{rel}(h2_3)=6.6\,\%$; $\theta_{rel}(h2_4)=2.0\,\%$; $\theta_{rel}(h2_m)=20.5\,\%$ (with varying m). Domain sizes are: $A(d2)=(4208\pm3615)$ nm^2; $A(h2_2)=(1858\pm1044)$ nm^2; $A(h2_3)=(1571\pm1005)$ nm^2; $A(h2_4)=(1615\pm812)$ nm^2; $A(h2_m)=(2377\pm1251)$ nm^2 (with varying m). However, these are first data and do not allow an interpretation of the phase behavior with regard to concentration, temperature, and ripening effects. Details are given in the Supporting Information.

[16] Alkoxy side chains that do not contribute to the packing but are either randomly adsorbed or point into the solution phase are not shown.

[17] As a result, we can compel another arrangement for the polycyclic heteroaromatic stars with -$OC_{16}H_{33}$ side chains from the *h*1 packing (shown in Figure 3b) to a packing similar to $h2_2$ (Figure 4a) by chemically adjusting the coordination number. $[\mathbf{2}]_{16}$ does not form a trimeric superstructure, because most probably the position at which the alkoxy chains are attached differs from the positional requirement for the trimer formation in $[\mathbf{1}]_{12}$; see the Supporting Information.

[18] a) G. Schull, R. Berndt, *Phys. Rev. Lett.* **2007**, *99*, 226105; b) Y. Wei, S. W. Robey, J. E. Reutt-Robey, *J. Phys. Chem. C* **2008**, *112*, 18537.

